Journal of Instrumentation

Performance study of a real-size mosaic high-rate MRPC

To cite this article: P. Lyu *et al* 2018 *JINST* **13** P06016

Published by IOP Publishing for Sissa Medialab

Received: *April 24, 2018*
Accepted: *June 8, 2018*
Published: *June 19, 2018*

Performance study of a real-size mosaic high-rate MRPC

P. Lyu,[a] D. Han,[a] Y. Wang,[a,1] B. Guo,[a] F. Wang,[a] X. Chen,[a] Y. Yu,[a] Y. Li,[a] L. Naumann,[b] A. Lazo Garcia,[b] D. Stach[b] and X. Fan[b]

[a] *Key Laboratory of Particle and Radiation Imaging, Department of Engineering Physics, Tsinghua University (Ministry of Education), Qinghuayuan No. 1, Beijing, China*

[b] *Helmholtz-Zentrum Dresden-Rossendorf, HZDR, Bautzner Landstraße 400, Dresden, Germany*

E-mail: yiwang@mail.tsinghua.edu.cn

Abstract: Towards the future CMS RPC upgrade, a real-size mosaic high-rate MRPC has been designed and developed by Tsinghua University. The prototype is a 5-gap counter composed of the low-resistive glass. Because the maximum size of this glass cannot exceed $330 \times 280\,\text{mm}^2$, 6 regions of glass stacks are mosaicked together in order to achieve a large active area. This prototype was tested in HZDR-ELBE with 30 MeV e-beam. It shows an efficiency above 95% at the rate of $2\,\text{kHz/cm}^2$. The time resolution is around 55 ps, and the cluster size is below 1.5. The performance is almost unaffected by increasing the rate to $11\,\text{kHz/cm}^2$. This design is proved to be fully capable of the CMS upgrade requirement by this HZDR beam test. The mosaic technology will make the high-rate MRPC a good choice in large-area timing systems.

Keywords: Performance of High Energy Physics Detectors; Resistive-plate chambers; Instrumentation and methods for time-of-flight (TOF) spectroscopy

2018 JINST 13 P06016

[1] Corresponding author.

https://doi.org/10.1088/1748-0221/13/06/P06016

Contents

1 Introduction

The multi-gap resistive plate chamber (MRPC) is a kind of gaseous detector first developed by ALICE Collaboration at CERN in 1996 [1], with much improved timing ability and equal detecting efficiency compared to the RPCs. It has become a promising candidate as timing detector widely in the high-rate nuclear and particle physics experiments. In the near future, the Compact Muon Solenoid (CMS) experiment [2], one of the general purpose detectors built at the Large Hadron Collider (LHC), intends to upgrade its detector systems to continue with the vast physics program at the high luminosity LHC. As part of the muon system, the trigger RPCs are expected to sustain a particle flux rate up to several dozens of kHz/cm^2 in the scenario of the LHC luminosity going up to $10^{34–35}$ cm^{-2}s^{-1} [3]. The design of these endcap RPCs applies a double High Pressure Laminate (HPL) gas gap, varnished with the linseed oil on the inner surface to reduce the noise rate [4]. However, the present system does not have the necessary redundancy to control the trigger rate at the increased luminosity while preserving high trigger efficiency [3]. Thanks to the development of the low-resistive glass in recent years, the glass MPRC can be an ideal alternative in the upgrade with remained excellent performance even under extremely high flux rate [5, 6]. Its excellent timing ability can also help to discriminate muons from other particles. The only problem is the dimension of the high-rate MPRC is limited to 330×280 mm^2, which is the maximum size of the low-resistive glass owing to the composition and production technique. This is far from satisfactory with respect to the size requirement (1 m scale) of the CMS muon detector. A mosaic design that joints several regions of glass stacks would be a feasible solution.

Through years of study and experiments, we have developed several designs towards the mosaic interface. The first design jointed two pieces of glass together by glue [7]. The dark current of this design was very high during the CERN GIF++ beam test, and even reached 2.2 μA after the beam was stopped. This has been confirmed to be caused by the sparking around the glued interface. The second design jointed the glass pieces with a fishing line block [8], and it decreased the dark current to a normal value of 20 nA. However, when it was applied to the real-size situation where 6 groups of glass stacks should be jointed in a 2×3 fashion, the problems of fishing line overlapping and HV failure emerged. To solve these problems, we develop another design that joints the glass pieces together directly without any spacers between. The mechanical stability is ensured by the fixing blocks surrounded and the gas gap spacer. This indeed works with low dark current and noise rate. A real-size prototype based on such interface design was produced and tested.

This article is organized as follows: section 2 introduces the structure and parameter of the real-size mosaic MRPC, especially the mechanical system keeping all glass pieces together. Section 3 is devoted to the performance of this prototype in HZDR-ELBE beam test, including the data analysis strategy and results. Section 4 summarizes the conclusions and outlooks.

2018 JINST 13 P06016

2 Real-size mosaic high-rate MRPC

The real-size mosaic MRPC is a single-stack design with five 250 μm gas gaps. These gas gaps are divided by six layers of resistive plate composed of the low-resistive glass (10^{10} Ωcm of the bulk resistivity). The bottom and top layers are sprayed with the colloidal graphite as the high voltage electrode. The gas gaps are defined by the nylon monofilaments spacers (shown as the red line in figure 1) for a homogeneous gap width. To achieve a relatively large detecting area required by CMS endcap RPC system, the trapezoidal reading out PCB board is 450 mm at topline, 540 mm at baseline and 1020 mm at height. On each of them, the 44 trapezoidal (6 mm/8 mm) double-ended strips are on a 10 mm pitch with 3 mm interval. The signals induced with both polarities are sent in differential fashion to the NINO front-end-electronics [9]. It should be noticed that the impedance is not a constant value on the trapezoidal strip due to the varying width. Reflections on tiny scale happen along the strip continuously and pile up, leading to an output signal with lower amplitude and increased width. Anyhow, the impedance mismatch will never affect the leading edge of the signal, so it will do no harm to the counter's timing ability.

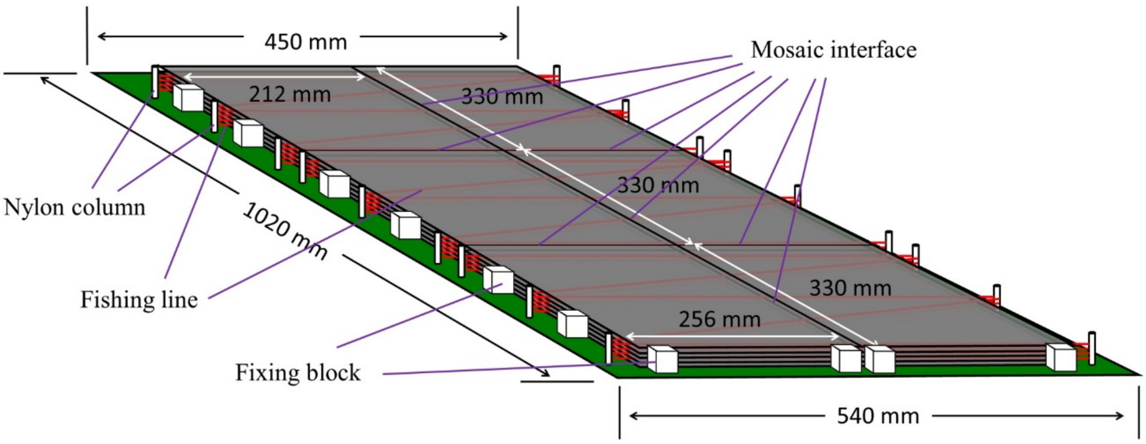

Figure 1. The sectional sketch of the real-size mosaic MRPC prototype with the glass plates jointed directly together without any spacers at the interface.

Because the low-resistive glass's dimension is restricted to be much smaller than the active area by its composition and processing technology, 6 stacks of the low-resistive glass plates are jointed together in a 2×3 way shown in figure 1. Instead of gluing the neighboring glasses or blocking them by fishing line, there is nothing at the joint interface for this prototype. The adjacent glass plates just get touched with each other directly. To keep the system mechanically stable, several blocks (the white blocks shown in figure 1) are fixed surrounding the outline of the whole 6 glass piles to make it stable overall. The fishing line (the red line shown in figure 1), which form the gas gaps, are strictly laid to press the 6 mosaic glass plates on each layer tightly still. When the top and bottom PCB are soldered together with pins, the glass stacks between will be pressed and stand still although there is no glue or anything at the interface. In the HV test, the dark current of this counter at the nominal voltage ±6800 V is around 20 nA, which proves that the design of the interface is feasible. The parameters of the counter are available in table 1.

Table 1. The parameters of the real-size mosaic MRPC prototype.

MRPC Parameter	Design Value/mm
Gas gap number	5
Gas gap width	250 μm
Glass thickness	700 μm
Glass bulk resistivity	$\sim 10^{10}\ \Omega$cm
Strip number	44
Strip width	6 mm/8 mm
Strip interval	3 mm
Strip length	1 m

3 HZDR beam test

3.1 Experimental setup

This real-size mosaic MRPC was tested at ELBE in HZDR with 30 MeV electron beam in March, 2017. The flux rate of the primary beam was tunable from a few electrons/s to 10^7 electrons/s [10]. The beam spot illuminating the MRPC was 100 mm in diameter. The MRPC was held in an aluminium gas box, working under a common gas mixture of 90% $C_2H_2F_4$, 5% i-C_4H_{10} and 5% SF_6, at a 60 mL/min flow rate.

The experimental setup is shown in figure 2. The tested MRPC module is fixed onto a movable platform, which allows us to select the beam spot's position on the counter. We set up a coordinate to control the beam spot's position on the MRPC module surface and define the detector plane center to be the zero point, shown in figure 3. For the test, the beam spot's center is placed to (−8 mm, −30 mm) on the coordinate. Restricted by the FEE channels, only the center 12 strips of the MRPC are tested. A laser calibrator helps to guarantee the beam spot's center is located between the 3rd and 4th strip among the 12.

A series of scintillators with different functions are set along the beamline. Among them, S1~4 are applied to define the coincidence trigger together with the RF signal, which is the radio frequency signal given by ELBE with accurate timing. The trigger dimension is $20 \times 20\ mm^2$. S24 and S25 in the front are used as rate monitors. The scintillators S13, S14 and S6 have relatively small size, and they are for the additional purpose of position selection.

2018 JINST 13 P06016

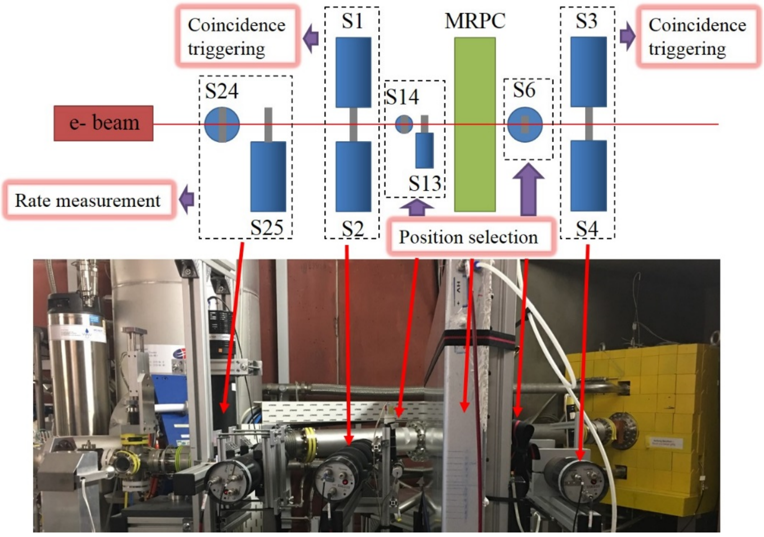

Figure 2. The skethc map and picture of the HZDR beam test experimenal setup. The MRPC and a scintillator chain are placed on the beam line. S1~4 are for coincidence triggering. S24~25 are for rate measurement. S6, S13~14 are for additional position selection.

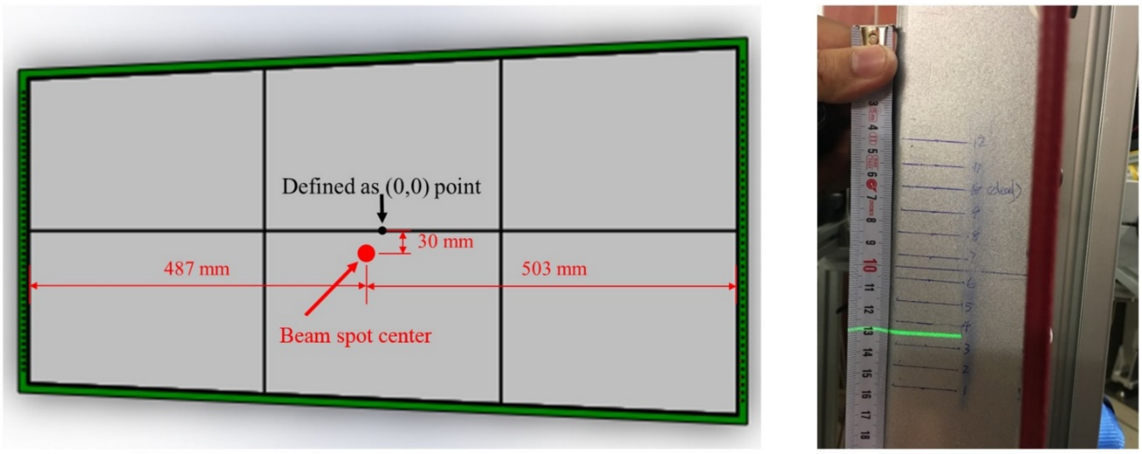

(a) (b)

Figure 3. To address the position of the beam spot on the MRPC module, a coordinate is setup and the center is defined as the zero point. (a) The beam spot's center is placed to (−8 mm, −30 mm) on the coordinate. (b) With the help of the laser calibrator, the beam spot center is ensured to be located between the 3rd and 4th strip among the 12 strips at center.

3.2 Data acquisition and analysis

As shown by the logical scheme of the DAQ chain in figure 4, three CAEN V1290 TDCs are applied for the DAQ. The scintillators' signals after the PMTs are fed into TDC0 (V1290N TDC in figure 4). The signals of the MRPC from NINO FEE will first go into a splitter board, and the timing information of the leading and trailing edge is recorded by TDC1 (V1290A TDC with positive input) and TDC2 (V1290A TDC with negative input) separately. The trigger signal is both fed into signal input of the 3 TDCs (black arrow in figure 4) besides the trigger input (red arrow in

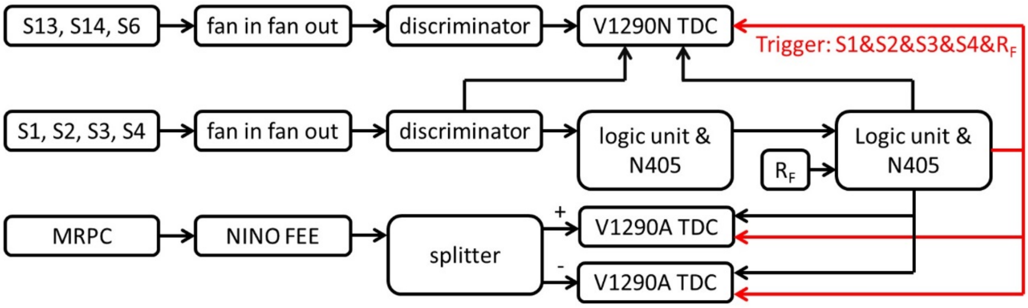

Figure 4. The logical scheme of the DAQ chain in the HZDR beamtest. The trigger signal is both fed into the trigger input and signal input of the 3 TDCs to work as a reference for synchronization.

figure 4) to work as a reference for synchronization. Thus the particle flight time between the RF signal and a single hit on the MRPC can be written to:

$$\mathrm{TOF} = \left(\frac{T_{\mathrm{LeftLead}} + T_{\mathrm{RightLead}}}{2} - T_{\mathrm{LeadRef}}\right) - (T_{\mathrm{RF}} - T_{\mathrm{Ref}}), \tag{3.1}$$

where T_{LeftLead} and $T_{\mathrm{RightLead}}$ are the time of the signal's leading edge readout on the left and right end of one MRPC strip from TDC1. Taking the average value of them will help to eliminate the influence of the position along the strip to the time information. T_{LeadRef}, T_{TrialRef} and T_{Ref} are the time of the same trigger signal readout from the first input channels of the 3 TDCs. Since there is no external clock signal, to synchronize each TDC, the arrival time of the trigger signal should be subtracted from every time readout value of the respective TDC. Before the TOF is calculated, a strip-alignment correction is carried out on $(T_{\mathrm{LeftLead}} + T_{\mathrm{RightLead}})/2$ of each strip to eliminate the additive constant on timing brought by the different cable length and response of electronic components.

Similarly, the time-over-threshold, which can represent each signal's amplitude, is defined:

$$\mathrm{TOT} = \left(\frac{T_{\mathrm{LeftTrial}} + T_{\mathrm{RightTrial}}}{2} - T_{\mathrm{TrialRef}}\right) - \left(\frac{T_{\mathrm{LeftLead}} + T_{\mathrm{RightLead}}}{2} - T_{\mathrm{LeadRef}}\right) \tag{3.2}$$

where $T_{\mathrm{LeftTrial}}$ and $T_{\mathrm{RightTrial}}$ are the time of the signal's trailing edge readout from TDC2. Signals with large TOT have an earlier arrival time, which will lead to a systematic error in the time domain. A slewing correction is carried out to calibrate out the influence of TOT. Before this, a gain correction is conducted on the TOT to remove the effect of different FEE channels' gain factors. Figure 5 shows the time distribution and time-TOT correlation before and after calibrations. It can be clearly noted that after the time-of-flight is no longer related with TOT, the time resolution gets much improved.

To get the intrinsic time resolution of the MRPC, the following equation is needed:

$$\sigma^2\,(\mathrm{TOF}) = \sigma^2\,(T_{\mathrm{MRPC}}) + \sigma^2\,(T_{\mathrm{RF}}), \tag{3.3}$$

where the $\sigma\,(T_{\mathrm{RF}})$ is 35 ps given by the accelerator radio-frequency.

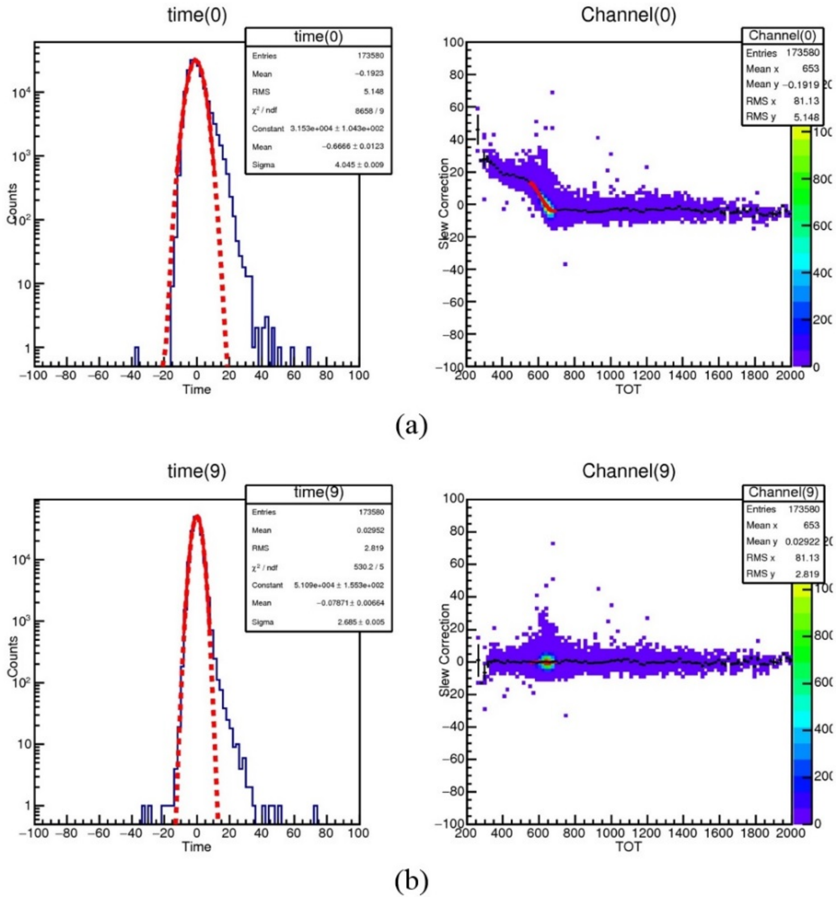

Figure 5. The raw time distribution and time-TOT correlation (a) and after calibration (b) in run 21. Calibrated with gain correction and slewing correction, the time-of-flight is no longer related with TOT. The time resolution gets improved from 101 ps to 67 ps (each bin on the time axis is 25 ps).

3.3 Test results and discussion

The HV scan was performed first at a rate of 11 kHz/cm^2. As shown in figure 6(a), the efficiency reaches 90% already at the HV of ±6600 V and is approaching to plateau region at ±6800 V. The cluster size increases with the applied HV because of the expanded avalanche, and it reaches 1.5 at ±6800 V (figure 6(b)). The time resolution is obtained after calibrations. For the first several runs (Run005~Run009), there were still a few setting problems in the TDCs, which can be observed from the time resolution's abnormally large values above the others in figure 6(c). After they were fixed, we got reasonable time resolution stable around 50 ps.

To study the rate capability of the mosaic MRPC, the detection efficiency was scanned under a series of different electron flux. As shown in figure 7(a), the efficiency curves under the flux rate of 0.35 kHz/cm^2 and 2.3 kHz/cm^2 almost coincide together, while the efficiency under 11 kHz/cm^2 is only slightly lower (about 1%). There is no efficiency loss at the rate of 2 kHz/cm^2, and the loss is negligible even the rate is increased to a level of 10 kHz/cm^2. The time resolution doesn't fluctuate much with the rate, always staying around 55 ps in figure 7(b).

2018 JINST 13 P06016

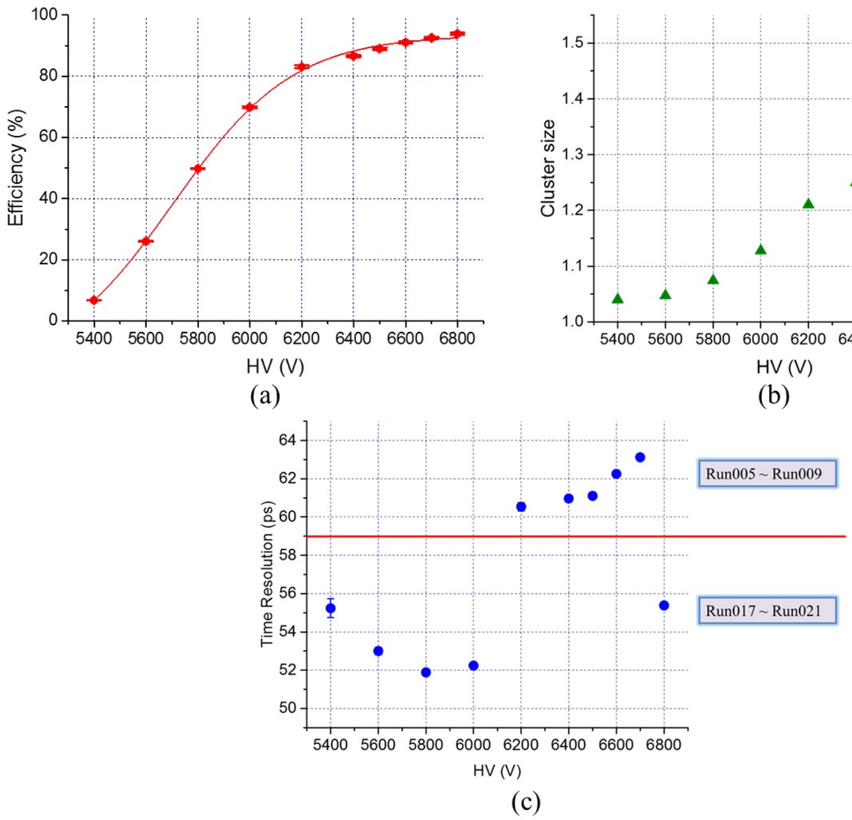

Figure 6. The performance of the mosaic MRPC in HV scan at the rate of 11 kHz/cm^2. (a) Efficiency. (b) Cluster size. (c) Time resolution.

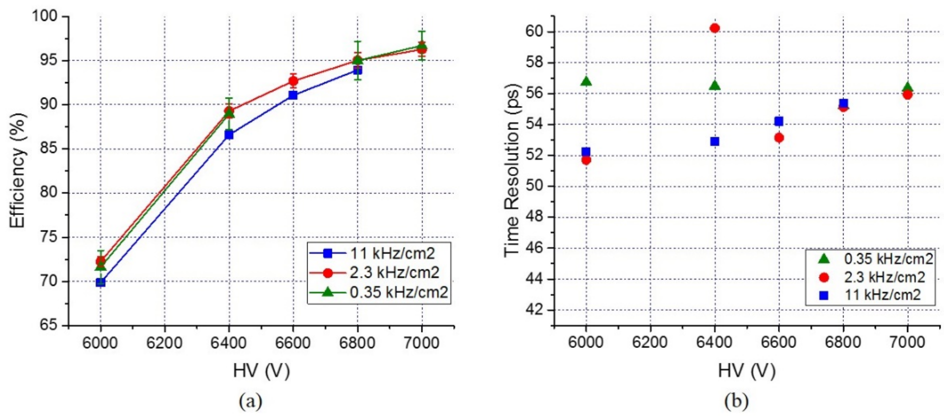

Figure 7. The performance of the mosaic MRPC in rate scan from 0.35 kHz/cm^2 to 11 kHz/cm^2. (a) Efficiency. (b) Time resolution.

2018 JINST 13 P06016

When we tried to go on the test with rate increased from 2 kHz/cm^2 to 5 kHz/cm^2, an accident occurred due to the wrong communication with the accelerator. This led to a sudden beam luminosity soaring and exposed the counter to an extremely high rate of 120 kHz/cm^2, which is far beyond its designed rate capability. The counter's current went up to 8 μA, and we believe this did irremovable damage to the counter. This thought was proved that fluorinated polymer deposition were found in large scale on the surface of the low-resistive glass plate when we opened the counter later. To make clear of the phenomenon, further study should be carried out on the plasma chemistry related to the low-resistive glass in the future. After the rate dropped back to 5 kHz/cm^2, this MRPC can't be performed normally with an efficiency loss by 30%. In terms of existing results, this mosaic MRPC's performance remains stable at the rate of 11 kHz/cm^2, and non-mosaic MRPC with similar parameters composed of the low-resistive glass remained such performance at a higher rate of 70 kHz/cm^2 as reported in our previous study [11]. It is believed that the real-size mosaic MRPC is capable to meet the requirements of the CMS RPC upgrade through the HZDR beam test.

4 Conclusion

For the upgrade of the CMS RPC system, a full-size trapezoidal high-rate mosaic MRPC is designed and produced. In order to achieve the detecting area required by CMS endcap RPC system, 6 piles of glass plates are mosaicked together in a 2×3 fashion. At the interface, neither glue nor fishing line blocks are applied. The alignment of the glass plates is ensured by the fixing blocks and nylon monofilaments spacers. The dark current of this MRPC is at a pretty low level of 20 nA. In the HZDR beam test under a particle flux rate of 0.35 kHz/cm^2, the mosaic MRPC has shown a promising performance of 95% efficiency and 55 ps time resolution. There is nothing changed in the performance at 2 kHz/cm^2, and the efficiency only loses 1% when the rate reaches 11 kHz/cm^2. The existing results have already proved the real-size mosaic MRPC to be a suitable candidate for high-flux-rate experiments including CMS upgrade. It is a pity that the mosaic MRPC is damaged in the HZDR beam test by accident. Part of the rate scan under extremely high rate and the position scan remain undone, which should be further conducted in the future.

Acknowledgments

This study is supported by National Key Programme for S&T Research and Development under Grant No. 2016YFA0400100, the Ministry of Science and Technology under Grant No. 2015CB856905 and National Natural Science Foundation of China under Grant No. 11420101004, 11461141011, 11275108.

References

[1] E. Cerron Zeballos et al., *A New type of resistive plate chamber: The Multigap RPC*, *Nucl. Instrum. Meth.* **A 374** (1996) 132.

[2] CMS collaboration, *The CMS Experiment at the CERN LHC*, 2008 *JINST* **3** S08004.

[3] M. Tytgat et al., *The Upgrade of the CMS RPC System during the First LHC Long Shutdown*, *PoS* **RPC2012** (2012) 063 [arXiv:1209.1979].

[4] M. Abbrescia et al., *Effect of the linseed oil surface treatment on the performances of resistive plate chambers*, *Nucl. Instrum. Meth.* **A 394** (1997) 13.

[5] J. Wang et al., *Development of high-rate MRPCs for high resolution time-of-flight systems*, *Nucl. Instrum. Meth.* **A 713** (2013) 40.

[6] Y. Wang, H. Chen, W.-C. Ding, J.-B. Wang, Y. Li and J. Cheng, *Progress of R&D and production of timing RPCs in Tsinghua University*, *Nucl. Instrum. Meth.* **A 661** (2012) S134.

[7] F. Wang et al., *Performance study of a Mosaic high rate MRPC*, 2016 *JINST* **11** C09016.

[8] F.-Y. Wang et al., *Performance study of new style mosaic MRPC*, *Chin. Phys.* **C 40** (2016) 116006.

[9] F. Anghinolfi et al., *NINO: An ultra-fast and low-power front-end amplifier/discriminator ASIC designed for the multigap resistive plate chamber*, *Nucl. Instrum. Meth.* **A 533** (2004) 183.

[10] L. Naumann et al., *Ceramics high rate timing RPC*, *Nucl. Instrum. Meth.* **A 628** (2011) 138.

[11] W. Zhu et al., *A real-size MRPC developed for CBM-TOF*, *Sci. China Technol. Sci.* **56** (2013) 2821.

2018 JINST 13 P06016